Quantum Electronics **48** (3) 283–289 (2018)

LASER GYROSCOPES

https://doi.org/10.1070/QEL16509

The nonmagnetic component of the zero bias of a Zeeman laser gyroscope

Yu.Yu. Kolbas, M.E. Grushin, V.N. Gorshkov

Abstract. **The physical reasons for time and temperature drifts of the nonmagnetic component of the zero bias of a Zeeman laser gyroscope are investigated. A study is made of the nonmagnetic zero bias as a function of temperature and discharge current in a Zeeman laser gyroscope; constructive and technological solutions to its reduction are proposed.**

Keywords: *laser gyroscope, Zeeman effect, nonmagnetic component of the zero bias.*

1. Introduction

In previous work [1–7], we considered drifts of the zero bias of a Zeeman laser gyroscope (ZLG), operating in the regime of switching of longitudinal generation modes with opposite circular polarisation (the so-called quasi-four-frequency regime or mode reversal), and methods for reducing the influence of the magnetic (caused by internal and external magnetic fields and depending on the direction of circular polarisation of the light wave) and partially nonmagnetic (independent of the magnetic fields and the direction of circular polarisation of the light wave) zero bias on the total error in measuring the angular velocity of rotation. We obtained an expression for the total error of the ZLG during its operation as a function of the mode switching period and derived equations describing the magnetic dynamic drift of the gyroscope at the instant of mode switching; methods for compensating such dynamic drifts were proposed [4]. It was found that the main contribution to the total error in such a ZLG is made by the nonmagnetic zero bias, and the additional drift associated with the mode reversal has a magnetic nature in the Zeeman gyroscope. The magnetic drift in the ZLG and methods of its compensation were considered in [8].

In this paper we study the physical reasons for the appearance of the nonmagnetic component of the zero bias in the ZLG, which are not related to the mode reversal, but are determined by the processes in the active gas-discharge medium of the ZLG. Quantitative errors are estimated and experimental data are obtained for the K-5 ZLG (OJSC M.F. Stel'makh Polyus Research Institute).

Yu.Yu.Kolbas, M.E. Grushin, V.N. Gorshkov Open Joint Stock Company M.F. Stel'makh Polyus Research Institute, ul. Vvedenskogo 3, korp. 1, 107342 Moscow, Russia; e-mail: tigra-e@rambler.ru

Received 31 August 2017; revision received 7 December 2017
Kvantovaya Elektronika **48** (3) 283–289 (2018)
Translated by I.A. Ulitkin

2. Physical reasons for the appearance of a nonmagnetic component of the zero bias of a Zeeman ring laser

For a ZLG, one can single out the following physical causes leading to a nonmagnetic component of the zero bias:

– quantum noise due to the finiteness of the resonator Q factor and the power stored in the resonator (the quantum limit of accuracy) [9, 10];

– change in dynamic lock-in zones depending on the amplitude of the frequency bias [11–14];

– change in the phase of the backscattering sources on the mirrors due to a change in the perimeter of the ZLG during self-heating or a change in the ambient temperature [15];

– noise in the output signal caused by the discrete nature of information reading from the ZLG [16];

– Langmuir zero bias associated with the asymmetry of the discharge channels and with the difference in currents in the arms of resonator, cataphoresis [5, 17, 18] and also thermal slip due to nonuniform heating of gas-discharge channels [19, 20], called nonmagnetic current zero bias; and

– nonlinear dependence on the time of the magnetic drift component leading to the emergence of an apparent change in the nonmagnetic drift component [21].

The theoretical limit of a minimum possible nonmagnetic zero bias $\Omega_{\rm gnm}$ is determined by spontaneous emission [9, 10]:

$$\Omega_{\rm gnm} = \frac{cL}{4S\nu_0}\sqrt{\frac{D_{\rm f}}{t}}, \;\; D_{\rm f} = \frac{32\pi^3 h\nu_0\Delta\nu_{\rm r}^2}{P}, \qquad (1)$$

where $D_{\rm f}$ is the spectral density of the fluctuations of the frequency difference of the counterpropagating laser waves at zero frequency; c is the speed of light; L is the perimeter of the resonator; S is the area covered by the optical contour; ν_0 is the frequency of laser generation; $\Delta\nu_{\rm r}$ is the resonator bandwidth; h is the Planck constant; P is the power of laser radiation inside the resonator; and t is the operating time in one longitudinal mode.

For the K-5 ZLG, the values of the parameters in (1) are as follows: $L = 0.2$ m, $S = 0.0025$ m^2, $\nu_0 = 4.73\times10^{14}$ Hz, $\Delta\nu_{\rm r} = 5.6\times10^5$ Hz, $P = 5\times10^{-2}$ W, $t = 60$ s , $h = 6.626\times10^{-34}$ J Hz^{-1} and $\Omega_{\rm gnm} = 0.0011$ deg h^{-1}.

The occurrence of dynamic lock-in zones in a laser gyro with a periodic frequency bias was first observed by V.N. Kuryatov [11] and investigated in detail by many authors [12–14, 21–24]. At the same time, two methods were suggested for their elimination: introduction of additional noise or substantially lower-frequency periodic frequency bias (a so-called slow meander). It was shown in [23] that the maximum desynchronisation efficiency is observed at the amplitude of an additional frequency bias, or the amplitude of a slow meander, equal to half the switching frequency of the bias. According to [18, 23] the nonmagnetic zero bias of the K-5 ZLG at a zero angular velocity ($\Omega_{\rm gnmL}$) is 0.0096 deg h^{-1} for the static lock-in zone $\Omega_{\rm L}$ of 100 Hz at a frequency bias amplitude of 50000 Hz, a bias switching period of 0.005 s, a bias switching front duration of 5×10^{-6} s, a slow meander amplitude of 100 Hz and a slow meander period of 1 s. To reduce the lock-in error, it is advisable to increase the slow meander switching period.

The nonmagnetic zero bias caused by backscattering sources ($\Delta\Omega_{\rm gr}$) was considered in [15]. The experimentally observed $\Delta\Omega_{\rm gr}$ value for the K-5 ZLG is 0.005 Hz, which, taking into account the scale factor, gives a zero bias of 0.014 deg h^{-1}.

The noise component of the output signal due to the discretisation of information is determined by the gyroscope discrete d, the time of operation in one mode t, and the total time of operation $t_{\rm w}$ [22]. Then, for the K-5 ZLG generating four pulses per period of the output signal, one can obtain the root mean square value of noise equal to $\sigma = 0.00074$ deg h^{-1} at $d = 0.69$ arcsec pulse^{-1}, $t = 60$ s and $t_{\rm w} = 3600$ s.

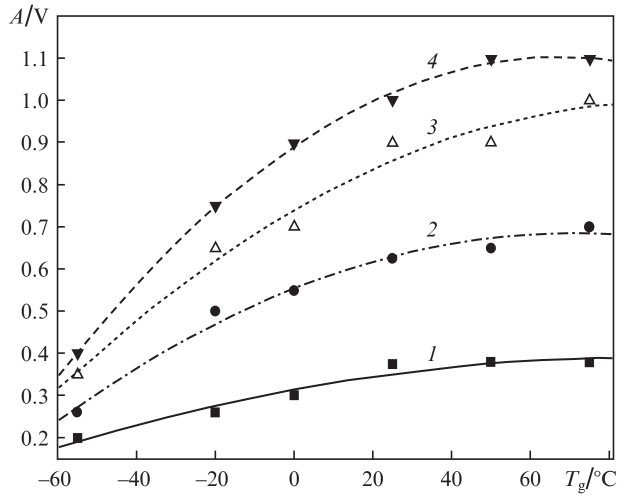

Figure 1. Dependences of the amplitude A of the K-5 ZLG output signal on the temperature of the working mixture $T_{\rm g}$ at the discharge current I = (*1*) 1.5, (*2*) 2, (*3*) 2.5 and (*4*) 3 mA. The radius of the channel is $R \approx 0.125$ cm, $p_0 = 5.4$ Torr at $T_{\rm g} = +25$°C, $\alpha = p_{\rm Ne}/p_{\rm He} = 0.07$. The discharge is sustained in one half of the ZLG.

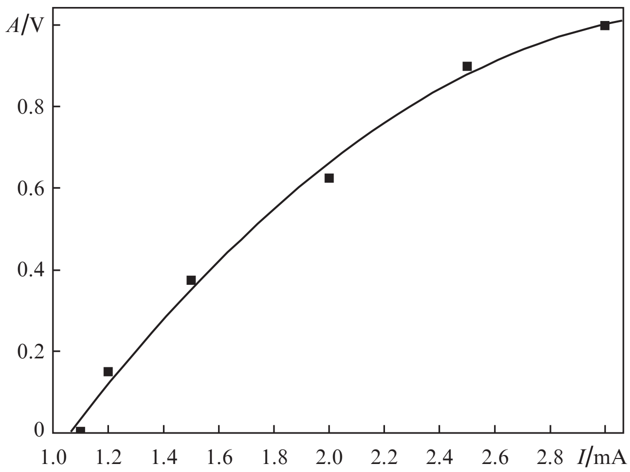

Figure 2. Dependence of the amplitude A of the K-5 ZLG output signal on the discharge current at an ambient temperature of +25°C; $R \approx 0.125$ cm, $p_0 = 5.4$ Torr, $\alpha = 0.07$. The discharge is sustained in one half of the ZLG.

3. Investigations of temperature and current dependences of the current zero bias of a Zeeman ring laser pumped by discharge in one half of the resonator

The current zero bias ($\Omega_{\rm gnmi}$) is based on the frequency shift of the centres of the gain curve of a gaseous medium for each of the counterpropagating waves during the motion of the gaseous medium and, accordingly, the pulling of counterpropagating waves to the new positions of the gain maxima.

According to [11–13], in the linear approximation the value of pulling for each of the waves '+' and '–' in the positive half-period of the bias switching ($\sigma_+^\pm$) can be written in the form

$$\sigma_+^\pm = \frac{G_0 cl}{\sqrt{\pi}L^2 u}\left(\pm\frac{c\Delta\nu}{\nu_0} \pm \vartheta\right), \qquad (2)$$

where G_0 is the gain at the centre of the gain curve; l is the length of the gas-discharge gaps; $u = (2kT/m)^{1/2}$ is the thermal velocity of motion of active neon atoms; m is the mass of the neon atom; k is the Boltzmann constant; $\Delta\nu$ is the value of the frequency splitting due to the Zeeman effect; $\nu_0 = c/\lambda$ is the frequency of laser generation; λ is the generation wavelength; and ϑ is the translational velocity of the active atoms.

Accordingly, during the switching period of the bias, the average beat frequency, i. e., the value of the current zero bias,

$$\Omega_{\rm gnmi} = \frac{\sigma_+^+ - \sigma_+^- + \sigma_-^+ - \sigma_-^-}{2} = -\frac{G_0 cl}{\sqrt{\pi}L^2 u}\vartheta. \qquad (3)$$

The gain G_0 depends on the discharge current, the pressure of the working mixture at $T = 25$°C (p_0) and the ratio of the pressures of helium and neon, as well as on the distance to the axis of the gas-discharge channel and the temperature of the working mixture.

Figures 1 and 2 show the experimental dependences of the value of the K-5 ZLG output signal on the temperature of the working mixture and the discharge current with the discharge sustained in one half of the resonator, and Fig. 3 demonstrates the dependence of the threshold generation current on the pressure of the working mixture.

It follows from the experimental curves presented in Figs 1–3 that $G_0 \sim I^{1/2}$, $T_{\rm g}^{1/2}$, $1/p_0$.

The expression for G_0 known from the literature gives a decreasing dependence on the pressure of the working mixture for $p_0 > 5$ Torr (shown in Fig. 4):

$$G_0 \approx 4.6\times10^{-6}\frac{\alpha p_0 I}{R^2}$$
$$\times\left(\frac{2p_0R(1-\alpha)^2}{4\alpha p_0^2R^2 + 0.0256(1+0.2p_0)(1+0.47p_0^2RI)} - 1\right)$$
$$\times\left(1-\frac{r^2}{R^2}\right), \qquad (4)$$

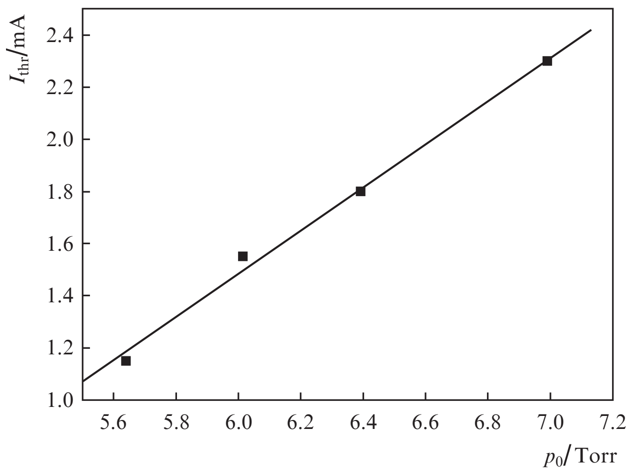

Figure 3. Dependence of the threshold generation current I_{thr} for the K-5 ZLG on the pressure of the working mixture at an ambient temperature of +25°C; $R \approx 0.125$ cm, $\alpha = 0.07$. The discharge is sustained in one half of the ZLG.

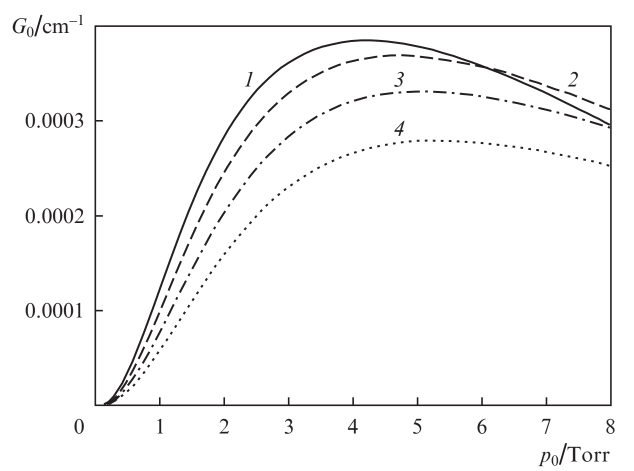

Figure 4. Dependences of the unsaturated gain G_0 calculated in accordance with formula (4) at the centre of the spectral line on the pressure of the working mixture at $R \approx 0.125$ cm, $I \approx 1$ mA and α = (*1*) 0.1, (*2*) 0.07, (*3*) 0.05 and (*4*) 0.035.

where r is the distance from the axis of the gas-discharge channel (the quantities G_0, I, p and R are measured in 1 cm^{-1}, mA, Torr and cm, respectively).

It should be noted that expression (4) does not reflect experimentally observed temperature and discharge current dependences of G_0 (see Figs 1, 2).

It was shown in [25] that the effective cross section for energy transfer from the metastable He ($2\,^1S_0$) level to the Ne ($3s_2$) level increases with increasing temperature. This should lead to an increase in G_0 with increasing gas temperature. However, the experimentally obtained root dependence of G_0 on the temperature indicates the predominance of the G_0 contribution in the temperature dependence caused by the depletion of the lower metastable level Ne ($1\,S_2$) due to diffusion of the excited Ne atoms on the tube wall. The longer the depletion time τ, the smaller the gain: $G_0 \sim 1/\tau$.

The diffusion rate increases with increasing gas temperature. Hence, $\tau \sim R/u_{dif} \sim T_g^{-1/2}$, where u_{dif} is the diffusion rate of the atoms. Thus, we obtain $G_0 \sim T_g^{1/2}$. To analyse the temperature and current dependences of the nonmagnetic drift, we can assume that

$$G_0 \sim T_g^{1/2} I^{1/2} / p_0. \tag{5}$$

Let us consider gas flows in a gas-discharge channel when the resonator is filled with a working mixture at a pressure p_0. According to [26, 27], in the positive column of the glowing discharge the channel walls are charged negatively. As a result, in a wall layer of thickness λ_i equal to the mean free path of the helium ion, all the ions go to the walls and transfer their mechanical momentum to them. Electrons, in turn, are repelled by the negative charge of the walls and transmit their momentum to the atoms of the gas, which as a result move towards the anode. In the centre of the channel, an equalising gas flow moves from the anode to the cathode. The zero bias caused by the particle motion is called the Langmuir zero bias. In addition, due to the effect of cataphoresis, an additional flow of gas from the cathode to the anode occurs. According to [28], the resulting pressure drop of the gas in the anode–cathode direction is described by the expression

$$\frac{\Delta p}{\Delta l} = 4.6 \times 10^{-3} \frac{I \lambda_i^3 \sqrt{U_e}}{\lambda_e R^5}\left(1 - \frac{9\lambda_i}{2R}\right) - 5 \times 10^{8} \frac{I b_i \eta \sqrt{U_e}}{n_g \lambda_e R^4} - 4 \times 10^{-9} \frac{E \ln\left(\dfrac{R}{2\lambda_i}\right) U_e}{R^2}, \tag{6}$$

where $U_e = 3/2kT_e$; T_e is the electron temperature (in eV); n_g is the concentration of gas atoms (in cm^{-3}); λ_e is the mean free path of an electron in helium [27] (in cm); b_i is the mobility of helium ions; E is the longitudinal electric field strength (V cm^{-1}); I is the discharge current (A); η is the viscosity of helium, determined by the formula [29]

$$\eta = 0.111 \frac{T_g^{3/2}}{T_g + 79.4} \ \ (\text{Torr s}^{-1}), \tag{7}$$

in which T_g is measured in kelvins; $\lambda_e p_0 = 0.08$ (cm); and $\lambda_i p_0 = 0.013$ (cm) [27].

The first term in Eqn (6) reflects the actual Langmuir zero bias, the second term – cataphoresis, and the third term takes into account the difference in ion and electron concentrations in the positive column of the gas discharge and, accordingly, the decrease in repulsion of electrons by the wall charge. The concentration of gas atoms is constant, although losses of up to 2% of helium are possible during the operation and storage of a ZLG (10–15 years).

The authors of [27, 28] present an experimental dependence of the product $b_i p_0$ on the ratio E/p_0, from which one can obtain

$$b_i \approx \frac{7980}{p_0} - 111.8 \frac{E}{p_0^2} \ \ (\text{cm}^2\ \text{V}^{-1}\ \text{s}^{-1}). \tag{8}$$

According to [29], the electron velocity and the electric field strength for helium are related by the expression

$$\frac{E}{p_0} \approx 0.292 U_e \ \ (\text{V cm}^{-1}\ \text{Torr}^{-1}). \tag{9}$$

Then expression (8) can be rewritten in the form

$$b_i \approx \frac{7980}{p_0} - 32.65\frac{U_e}{p_0}. \quad (10)$$

The concentration of the helium atoms, n_g (cm^{-3}), is related to the pressure p_0 (Torr) at $T_g = 273$ K by the expression [30]

$$n_g = 3.54 \times 10^{16} p_0. \quad (11)$$

After substituting expressions for $\lambda_i, \lambda_e, b_i, \eta, E$ into equation (6) with allowance for $\lambda_i \ll R$, we obtain

$$\frac{\Delta p}{\Delta l} = 1.2\times10^{-7}\frac{I\sqrt{U_e}}{p_0^2R^5} - 1.96\times10^{-8} \times\frac{I(7980-32.65U_e)T_g^{3/2}\sqrt{U_e}}{R^4(T_g+79.4)p_0} - 4\times10^{-9}\frac{E\ln\left(\frac{p_0R}{0.026}\right)U_e}{R^2}. \quad (12)$$

The electron temperature for helium depends on the radius of the gas-discharge channel and the pressure p_0 as follows [28]:

$$\sqrt{\frac{kT_e}{U_i}}\exp[U_i/(kT_e)] = 1.17\times10^7(Cp_0R)^2. \quad (13)$$

Here, $C = 4\times10^{-3}$, and $U_i = 24.6$ eV is the ionisation potential of helium.

Figure 5 shows the dependence of T_e on p_0R for helium, obtained using (13) in [28]. As follows from the figure, in the region of the ZLG values of $p_0R \approx 0.8-1$ Torr cm, the electron temperature rapidly decreases with increasing p_0R.

When the discharge is sustained in a closed volume, that is, at a constant concentration of the particles of the medium (as in the case of a ZLG), the electron temperature is determined only by the value of p_0R and does not depend on a change in the gas temperature. However, it has been experimentally established that an increase in T_g in the tests of the K-5 ZLG leads to an increase in the discharge voltage (Fig. 6). The increase in the discharge voltage can be associated with the loss of ions with increasing temperature. The mechanism of this effect requires additional studies.

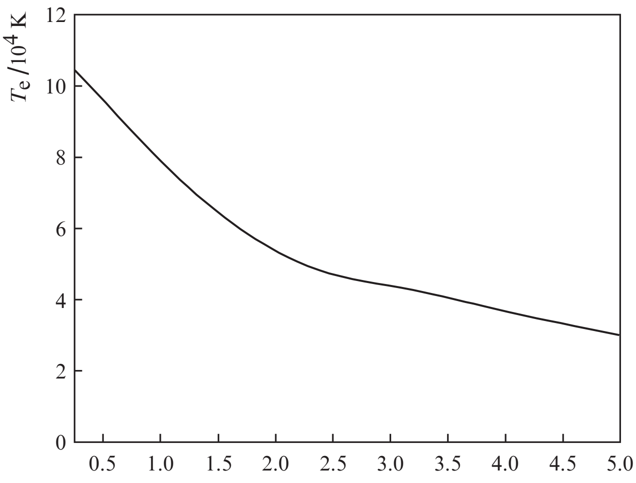

Figure 5. Dependence $T_e(p_0R)$ for He.

It follows from Fig. 6 that in analysing the temperature dependence of the gas pressure drop in the anode–cathode direction, we can assume

$$E(T),\ U_e \sim T_g. \quad (14)$$

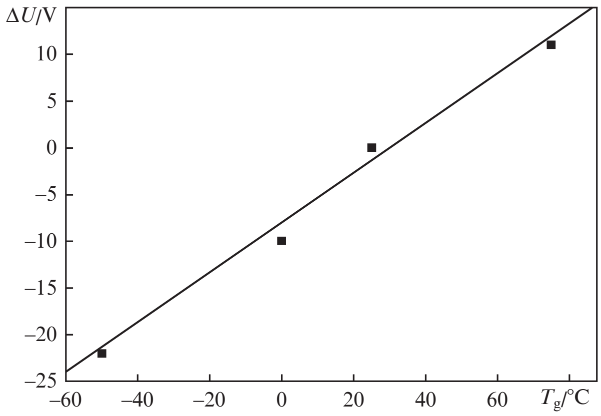

Figure 6. Change in the K-5 ZLG discharge voltage at a temperature in the range from −50 °C to +75 °C with respect to the voltage at room temperature. The discharge is sustained in one half of the ZLG, p_0 = 5.4 Torr.

According to the Poiseuille law, the directed velocity of the gas components depends on the distance r to the axis of the gas-discharge channel and the pressure drop as follows [30]:

$$\vartheta = \frac{1}{4\eta}(R^2 - r^2)\frac{\Delta p}{\Delta l}, \quad (15)$$

where η is the helium viscosity determined by formula (7).

For a fixed gas-discharge volume of the working mixture at a pressure p_0, by substituting (12) into formula (15), we obtain

$$\vartheta = \left(2.7\times10^{-7}\frac{I(T_g+79.4)\sqrt{U_e}}{T_g^{3/2}p_0^2R^5} - 4.41\times10^{-8}\frac{I(7980-32.65U_e)\sqrt{U_e}}{R^4p_0} - 10^{-9}\frac{(T_g+79.4)\ln\left(\frac{Rp_0}{0.026}\right)EU_e}{T_g^{3/2}R^2}\right)(R^2-r^2). \quad (16)$$

Thus, the gas flow rate decreases with increasing p_0 and R. The temperature dependence from (16), taking into account the above assumptions (14), can be represented as

$$v(T_g) = A - BT_g^{1/2} - CT_g^{3/2}. \quad (17)$$

If we take into account that $G_0 \sim T_g^{1/2}$ and $u \sim T_g^{-1/2}$, then it follows from (3) that the temperature dependence of the current zero bias $\Omega_{\text{gnmi}}(T_g)$ is determined by the dependence $v(T_g)$ (17).

Figure 7 shows the experimental dependences of the nonmagnetic zero bias $\Omega_{\rm gnm}$ on the temperature for the K-5 ZLG upon combustion of the discharge in one half of the ZLG, and also the results of their approximation by (17).

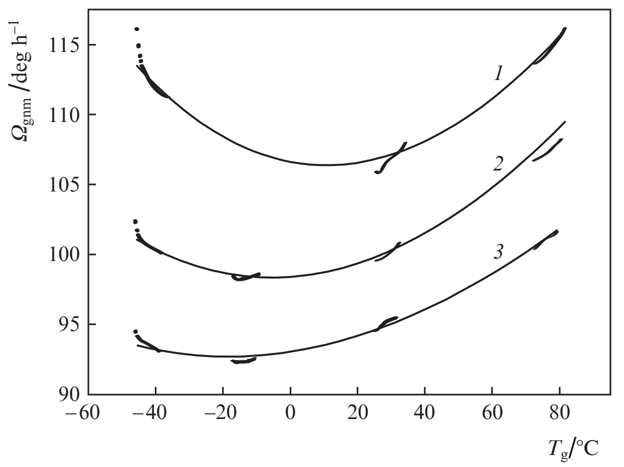

Figure 7. Experimental dependences $\Omega_{\rm gnm}(T_{\rm g})$ for the K-5 ZLG at p_0 = 5.4 Torr and currents I = (*1*) 3, (*2*) 2.4 and (*3*) 2 mA. The discharge is sustained in one half of the ZLG. Solid lines are the result of calculation by formula (17) at (*1*) $A = 552$, $B = 40$, $C = -0.05$; (*2*) $A = 407$, $B = 28$, $C = -0.03$; and (*3*) $A = 274$, $B = 20$, $C = -0.02$.

As can be seen from the results of the approximation, the nonmagnetic zero bias is completely determined by the current bias. It also follows from Fig. 7 that expression (17) for the gas flow rate v describes well the temperature dependence of the nonmagnetic zero bias of the K-5 ZLG. The largest contribution is made by the Langmuir zero bias (the first term) and cataphoresis (the second term). However, it should be noted that the sign in front of the third term in (17) is positive as a result of the approximation. This means that in addition to the mechanisms proposed in [28], additional processes, in particular, dissociative recombination of the neon ions, can contribute to the pressure drop between the anode and the cathode [see (6)] [31].

To determine the dependence $\Omega_{\rm gnmi}(I)$, it is necessary to take into account the dependence $U_{\rm e}(I)$. Figure 8 shows the current–voltage characteristic of the discharge in the K-5 ZLG. The solid line in the figure is the result of calculation of $U \sim 1/I$.

It follows from Fig. 8 that E/N, and hence $U_{\rm e}(I)$ are proportional to $1/I$. Taking (3) and (16) into account, we have

$$\Omega_{\rm gnmi}(I) = k_1 I + k_2/I^{3/2} + k_3, \tag{18}$$

where k_1 is the coefficient including the current dependences of the Langmuir drift and cataphoresis; k_2 is the coefficient of the current dependence of the difference between the concentrations of ions and electrons in the positive column of the gas discharge; and k_3 is the coefficient of thermal slip due to temperature difference.

Figures 9 and 10 show the experimental dependences $\Omega_{\rm gnm}(I)$ for two samples of the ZLG at $T_{\rm g}$ = +25 °C and $T_{\rm g}$ = +75 °C and the results of their approximation by formula (18). The figures demonstrate good agreement between the experimental data and the calculated curves. Note also that

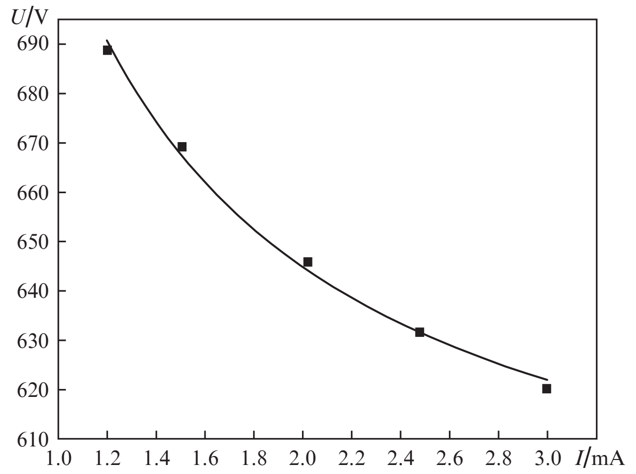

Figure 8. Current–voltage characteristic of the discharge in the K-5 ZLK. The discharge is sustained in one half of the ZLG.

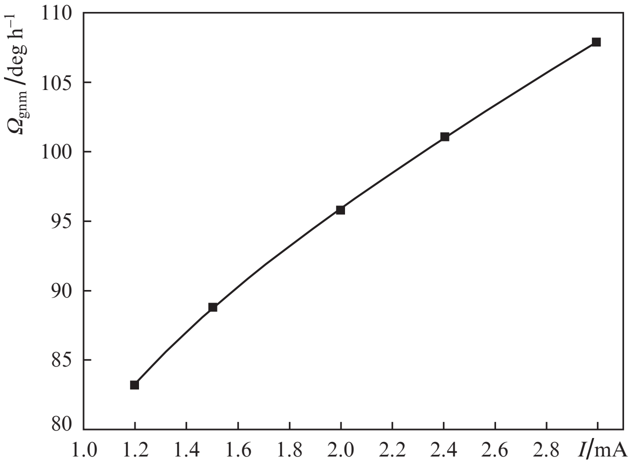

Figure 9. Dependence $\Omega_{\rm gnm}(I)$ for the K-5 ZLG at $T_{\rm g}$ = +25°C, p_0 = 5.4 Torr. The discharge is sustained in one half of the ZLG. The solid curve is the result of the calculation by formula (18) for k_1 = 10.3 deg (h mA)$^{-1}$, k_2 = −10.8 deg (h mA$^{3/2}$)$^{-1}$ and k_3 = 79 deg h^{-1}.

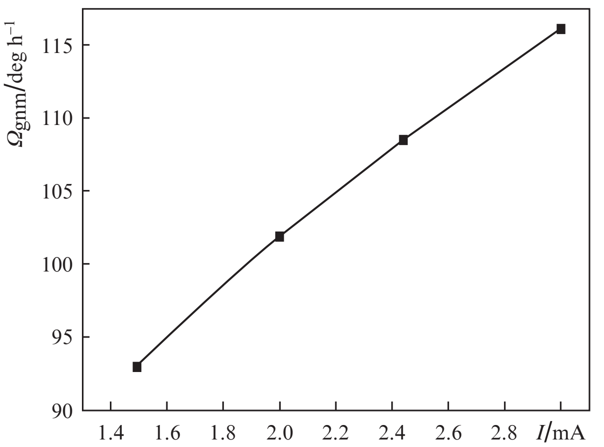

Figure 10. The dependence $\Omega_{\rm gnm}(I)$ for the K-5 ZLG at $T_{\rm g}$ = +75°C, p_0 = 5.4 Torr. The discharge is sustained in one half of the ZLG. The solid curve is the result of the calculation by formula (18) at k_1 = 11.8 deg (h mA)$^{-1}$, k_2 = −15 deg (h mA$^{3/2}$)$^{-1}$ and k_3 = 83.6 deg h^{-1}.

the coefficient in the dependence of the nonmagnetic zero bias on the discharge current [$\Omega_{\rm gnm} \approx \varkappa(I)$] is 0.014 deg h^{-1} μA^{-1}.

4. Temperature and current dependences of the current nonmagnetic zero bias of a Zeeman ring laser pumped by discharge in two 'counterpropagating' gas-discharge gaps

To compensate for the current zero bias, two gas-discharge channels of length l_1 and l_2 are installed in the ring laser. Their currents are approximately equal in magnitude and opposite in sign. As a result, the value of the current zero bias

$$\Omega_{\rm gnmi} = -\frac{(G_{01} - G_{02})c(l_1 - l_2)}{\sqrt{\pi}L^2 u}(\vartheta_1 - \vartheta_2). \qquad (19)$$

The absolute value of $\Omega_{\rm gnmi}$ is determined by the quality of the ZLG body (the same lengths of the gas-discharge channels and their diameters and the quality of the ZLG alignment), as well as the currents in the gas-discharge gaps (their absolute values and difference).

Figure 11 shows the dependence of the nonmagnetic component of the ZLG zero bias on the discharge current in two gas-discharge channels at different gas temperatures $T_{\rm g}$.

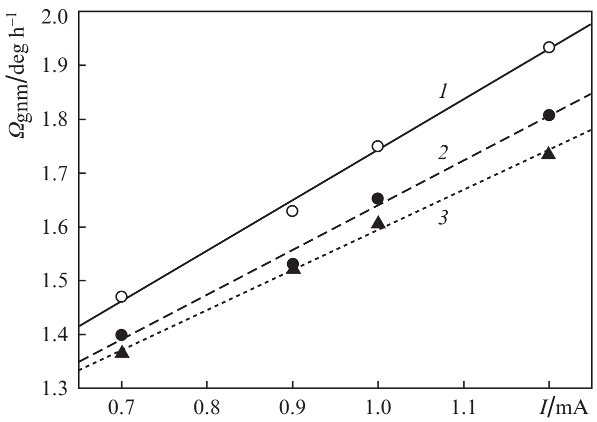

Figure 11. Dependence of the nonmagnetic component of the K-5 ZLG zero bias on the discharge current in two gas-discharge gaps at p_0 = 5.4 Torr and $T_{\rm g}$ = (*1*) −55 °C, (*2*) +25 °C and (*3*) +75 °C. The currents in the gaps are equal in magnitude and opposite in direction.

When the laser beam passes through the centre of the gas-discharge channel, two 'opposite' gas-discharge gaps make it possible to obtain the minimum dependence of the zero bias on the temperature $T_{\rm g}$ (Fig. 12). As the discharge current decreases, the temperature dependence of the nonmagnetic component of the zero bias is also reduced (Fig. 13).

As can be seen from Figs 12 and 13, the coefficients in the dependences of the nonmagnetic component of the ZLG zero bias on the temperature ($\Omega_{\rm gnm} = \varkappa_1 T_{\rm g}$) and the current ($\Omega_{\rm gnm} = \varkappa_2 I$) do not exceed 0.0003 deg (h °C)$^{-1}$ and 0.0002 deg (h μA)$^{-1}$, respectively.

Let us consider the causes and possible values of the error of the nonmagnetic component of the zero bias, expressed in the nonreproducibility of the nonmagnetic component, that is, in its incomplete compensation with the use of temperature correction. One of the reasons can be related to the shift of the

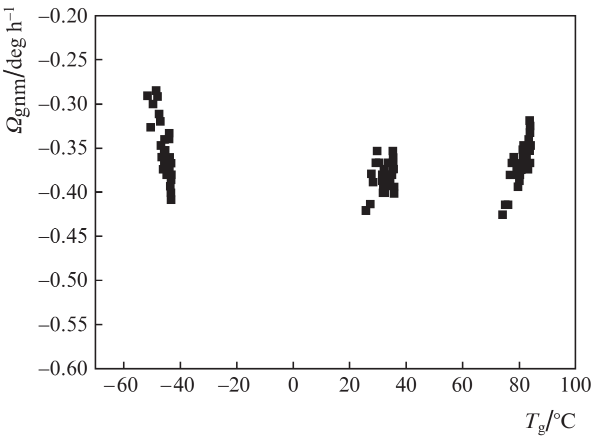

Figure 12. Temperature dependence of the K-5 ZLT nonmagnetic zero bias at p_0 = 5.4 Torr and I = 1.2 mA. The currents in the discharge gaps are directed towards each other.

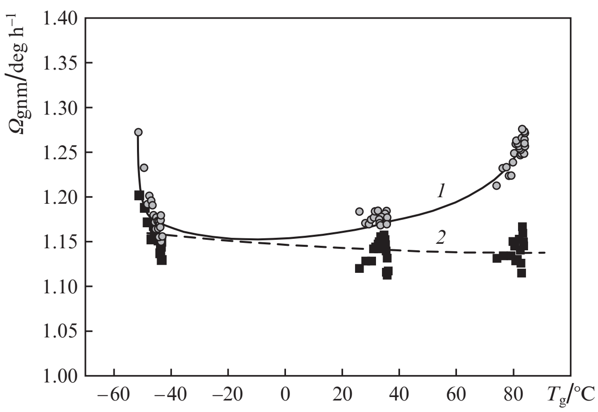

Figure 13. Temperature dependence of the K-5 ZLG nonmagnetic zero bias at I = (*1*) 1.2, (*2*) 0.7 mA and p_0 = 5.4 Torr. The currents in the discharge gaps are directed towards each other.

laser beam along the channel cross section. The position of the beam relative to the axis of the gas-discharge channel is determined during the resonator alignment. In a precisely fabricated and aligned resonator, the beam passes strictly along the axis of the gas-discharge channel. However, in practice this is not the case, and since the radius of the diaphragm of the ZLG resonator is usually chosen equal to twice the radius of the beam in the channel r_1, it is possible to shift the beam from the axis of the gas-discharge channel by a value close to r_1 (in the K-5 ZLG r_1 = 0.25 mm at R = 1.25 mm). Let us estimate the possible error due to the difference in the beam shifts relative to the axis of the gas-discharge channel. In the K-5 ZLG, the current nonmagnetic zero bias with one gas-discharge gap is ~ 100 deg h^{-1} at r_1 = 0.25 mm, R = 1.25 mm. Accordingly, from formulas (16) and (19) we obtain $\Omega_{\rm gnmi}$ = 8 deg h^{-1}.

The temperature dependence of $\Omega_{\rm gnmi}$, its reproducibility after temperature cycles and the ZLG stability in the process of its operation and storage are important for the practical application of a ZLG. We should emphasise that the laser beam practically does not change its position during self-heating of the device. The thermal expansion of the loop is uniform, and the compensation for this thermal expansion is effected by the displacement of only two mirrors. As a result, the beam is shifted along the channel cross section. During the self-heating time, an increase in the laser perimeter (lengthening) is taken to be $\Delta L = k_{\rm exp}TL$, where L is the perimeter and $k_{\rm exp}$ is the thermal expansion coefficient of the resonator body material. If the initial shape of the resonator is considered symmetrical, we can assume that to compensate for ΔL, each of the two piezo-mirrors should move to a distance $\Delta L/\sqrt{32}$; therefore, the maximum shift Δr of the beam along the channel cross section is $\sim L/8$.

For the K-5 ZLG at $r_1 = 0.25$ mm, $R = 1.25$ mm, $L = 200$ mm, $k_{\rm exp} = 1.5 \times 10^{-7}\,{}^{\circ}{\rm C}^{-1}$ and $\Delta T = 20\,{}^{\circ}{\rm C}$, the beam shift will be 7.5×10^{-5} mm, which is negligible is small in comparison with both the radius of the beam and the radius of the channel.

The shift of the beam along the channel cross section can result from the rotation of the mirror caused by local nonuniform heating. However, such an event is unlikely, since mirror designs are made thermally compensated and their reflective surface is capable of only parallel displacement [32]. Also, the values of L, l_1 and l_2 hardly depend on the temperature.

Thus, the nonreproducibility of the current zero bias can only be caused by the unreproducibility of the discharge currents and the imbalance of the discharge currents in the two arms, as well as by the change in the gas composition in gas-discharge channels (both total pressure and helium–neon ratio). For short-term nonreproducibility of the current zero bias, only the change in the discharge currents in the two arms – the imbalance of the discharge currents – is important. Since modern current stabilisers have an error of no more than $\pm 0.2\ \mu$A, the expected nonreproducibility of the current zero bias will not exceed 0.003 deg h^{-1}.

5. Conclusions

The nonmagnetic zero bias is the main reason limiting the ZLG accuracy. The main contribution to the zero bias is made by two components – backscattering of light on the mirrors and current drift. The most effective way to reduce the lock-in zones is to use a frequency bias with a minimum duration of the switching fronts and with an additional low frequency (slow meander) signal superimposed on it, followed by subtraction of the slow meander signal from the ZLG output signal. The residual value of the nonmagnetic zero bias due to backscattering in the K-5 ZLG is 0.014 deg h^{-1}.

The current drift significantly exceeds all other components of the nonmagnetic drift, reaching 1.3 deg h^{-1} in the K-5 ZLG. This value depends linearly on the length of the gas-discharge gaps and the discharge current and as $1/R^5$ on the radius of the gas-discharge gaps. However, the instability of the current zero bias is small (no more than 0.003 deg h^{-1}) and is determined only by the stability of the discharge current, which makes it possible to effectively use algorithmic temperature correction.

The total achieved error level of the nonmagnetic component of the ZLG zero bias does not exceed 0.016 deg h^{-1}.

References

1. Dmitriev V.G., Golyayev Yu.D., Vinokurov Yu.A., Kolbas Yu.Yu., Tikhmenev N.V. *Materialy 15-y Mezhdunarodnoy konferentsii po integrirovannym navigatsionnym sistemam* (Proc. 15 Int. Conf. 'Integrated Navigation Systems') (S.-Petersburg: TsNII Elektropribor, 2008) p. 127.
2. Golyaev Yu.D., Dmitriev V.G., Kazakov A.A., Kolbas Yu.Yu., Nazarenko M.M., Tikhmenev N.V., Yakushev A.B. Patent of Russian Federation No. 2408844, the priority of 07.10.2009.
3. Vinokurov Yu.A., Golyaev Yu.D., Dmitriev V.G., Kazakov A.A., Kolbas Yu.Yu., Tikhmenev N.V., Yakushev A.I. Patent of Russian Federation No. 2418266, the priority of 11.01.2010.
4. Vakhitov N.G., Golyaev Yu.D., Dronov I.V., Ivanov M.F., Kolbas Yu.Yu., Krutikov A.P. *Vestn. Mosk. Gos. Tekh. Univ. im. N.E. Baumana, Ser. Priborostroen.*, **2** (95), 10 (2014).
5. Golyaev Yu.D., Dronov I.V., Kolbas Yu.Yu., Pryadein V.A., Shpikalov B.N. *Vestn. Mosk. Gos. Tekh. Univ. im. N.E. Baumana, Ser. Priborostroen.*, **3** (88), 112 (2012).
6. Golyaev Yu.D., Ivanov M.A., Kolbas Yu.Yu., Krutikov A.P., Aristarkhova M.A., Belov A.V., Solovyova T.I. *Setevoi Elektronnyi Nauchn. Zh. 'Sistemotekhnika'*, **10**, 48 (2012).
7. Kolbas Yu.Yu., Ladonkina M.V., Solov'eva T.I. *Kachestvo. Innovatsii. Obrazovanie*, **3** (118), 35 (2015).
8. Kolbas Yu.Yu., Savel'ev I.I., Khokhlov N.I. *Quantum Electron.*, **45** (6), 573 (2015) [*Kvantovaya Elektron.*, **45** (6), 573 (2015)].
9. Klimantovich Yu.L. (Ed.) *Volnovye i fluktastionnye protsessy v lazerakh* (Wave and Fluctuation Processes in Lasers) (Moscow: Nauka, 1974).
10. Golyaev Yu.D., Kolbas Yu.Yu. *Quantum Electron.*, **42** (10), 949 (2012) [*Kvantovaya Elektron.*, **42** (10), 949 (2012)].
11. Kuryatov V.N., Landa P.S., Lariontsev E.G. *Izv. Vyssh. Uchebn. Zaved., Ser. Radiofiz.*, **11**, 1839 (1968).
12. Khoshev I.M. *Sov. J. Quantum Elelctron.*, **10** (5), 544 (1980) [*Kvantovaya Elektron.*, **7** (5), 953 (1980)].
13. Golyaev Yu.D., Kolbas Yu.Yu., Tikhmenev N.V., Khokhlov N.I. *Elektron. Tekh., Ser. 11. Lazer Tekh. Optoelektron.*, No. **4** (40), 34 (1986).
14. Khromykh A.M. *Elektron. Tekh., Ser. 11. Lazer Tekh. Optoelektron.*, No. **2** (53), 44 (1990).
15. Hurst R.B., Rabeendran N., Schreiber K.U., Wells J.-P.R. *Appl. Opt.*, **53** (31), 7610 (2014).
16. Golyaev Yu.D., Kolbas Yu.Yu. *Zh. Tekh. Fiz.*, **17** (8), 162 (1991).
17. Aronowitz F., in *Laser Applications*. Ed. by M. Ross (New York: Acad. Press, 1971).
18. Seregin V.V., Kukuev R.M. *Lazernye girometry i ikh primenenie* (Laser Gyrometers and Their Application) (Moscow: Mashinostroenie, 1990).
19. Privalov V.E. *Gazorazryadnye lazery v izmeritel'nykh sistemakh* (Gas-discharge Lasers in Measuring Systems) (Leningrad: Sudostroenie, 1989).
20. Grew K.E., Ibbs T.L. *Thermal Diffusion in Gases* (Cambridge: Cambridge University Press, 1951; Moscow: Fizmatiz, 1956).
21. Golyaev Yu.D., Kolbas Yu.Yu., Solovyova T.I. *Lazernyi girokompas na zeemanovskom kol'tsevom lazere. Metodicheskie ukazaniya* (Laser Gyrocompass based on a Zeeman Ring Laser. Methodical Guidelines) (Moscow: Izd-e MIEM NIU VShE, 2013) p. 43.
22. Golyaev Yu.D., Kolbas Yu.Yu., et al. *Sov. J. Quantum Electron.*, **20** (1), 80 (1990) [*Kvantovaya Elektron.*, **17** (1), 92 (1990)].
23. Golyaev Yu.D., Telegin G.I., Tolstenko K.A., Yaremenko S.O. *Elektron. Tekh., Ser. 11. Lazer Tekh. Optoelektron.*, No. 4 (56), 17 (1990).
24. Golyaev Yu.D., Kolbas Yu.Yu., Tolstenko K.A., Naida O.N., Chubar' A.V. *Elektron. Tekh., Ser. 11. Lazer Tekh. Optoelektron.*, No. 4 (52), 29 (1989).
25. Prokhorov A.M. (Ed.) *Spravochnik po lazeram* (Reference Book on Lasers) (Moscow: Sov. Radio, 1978).
26. Brown S. *Elementary Processes in Gas Discharge Plasma* (Cambridge, MA: MIT Press, 1959; Moscow: Atomizdat, 1961).
27. Raizer Yu.P. *Gas Discharge Physics* (New York: Springer, 1991; Moscow: Nauka, 1992).
28. Granovskii V.L. *Elektricheskii tok v gaze. Ustanovivshiisya tok* (Electric Current in Gas. Steady-state Current) (Moscow: Nauka, 1971).
29. Smits A.J., Dussauge J.-P. *Turbulent Shear Layers in Supersonic Flow* (Munich: Springer Science Business Media Inc., 2006) Vol. 14, p. 410.
30. Kasatkin A.G. *Osnovnye protsessy i apparaty khimicheskoi tekhnologii* (Main Processes and Apparatus of Chemical Technology) (Moscow: Izd-e GKhI, 1961).
31. Vinogradov V.I. *Opt. Spektrosk.*, **6** (110), 1042 (2011).
32. Zapotyl'ko N.R., Katkov A.A., Nedzvetskaya A.A. *Opt. Zh.*, **78**, 10 (2011).